International Journal of CAD/CAM Vol. 7, No. 1, pp. 11~20 (2007)

INTERNATIONAL JOURNAL OF CAD/CAM
www.ijcc.org

Smooth Boundary Topology OptimizationUsing B-spline and Hole Generation

Soobum Lee*, Byung Man Kwak and Il Yong Kim[†]

Postdoctoral Research Associate Department of Mechanical Engineering 1174 Engineering Lab. University of Maryland College Park, MD 20742 USA

[†]Department of mechanical and materials engineering, Queen's University, Kingston, Canada

Abstract – A topology optimization methodology, named "smooth boundary topology optimization," is proposed to overcome the shortcomings of cell-based methods. Material boundary is represented by B-spline curves and their control points are considered as design variables. The design is improved by either creating a hole or moving control points. To determine which is more beneficial, a selection criterion is defined. Once determined to create a hole, it is represented by a new B-spline and recognized as a new boundary. Because the proposed method deals with the control points of B-spline as design variables, their total number is much smaller than cell-based methods and it ensures smooth boundaries. Differences between our method and level set method are also discussed. It is shown that our method is a natural way of obtaining smooth boundary topology design effectively combining computer graphics technique and design sensitivity analysis.

Key Words **: Smooth boundary topology optimization, Selection criterion, B-spline, Topological sensitivity**

1. Introduction

The concept of topology optimization is motivated to determine the layout of a structure by changing the number of holes and the boundary shape. This research area began with a cell-based approach where the parameters of each design cell (which is often represented by a finite element) are determined. Bendsoe and Kikuchi utilized a homogenization method for structural optimization [4]. This method computes the macroscopic material properties by changing the parameters of the size and the orientation of each microvoid. Yang and Chaung [36] described a relationship between the density and elastic modulus using an empirical formula which is known as solid isotropic material with penalization (SIMP) [5,24]. An approach that removes design cells in a structure was also proposed. One of the simple ways is to remove the finite elements iteratively where the minimum stress values are detected. Xie et al. [7,18,31,35] introduced this methodology with the name, "evolutionary structural optimization (ESO)." Another method that removes finite elements based on the sensitivity analysis was also attempted. A topological sensitivity was introduced by Sokolowski and Zochowski [27]. An infinitesimal hole is introduced in a domain and a topological sensitivity defined as the perturbed amount of a cost function divided by the volume of the infinitesimal hole. The "hard kill" method was proposed [22] by eliminating finite elements with small topological sensitivities. Other ways of defining topological sensitivities were found in Novotny et al. [22] and Garreau et al. [11].

*Corresponding author:
Tel: +1-301-405-3871 (Office)
Fax: +1-301-300-8942 (Cell)
E-mail: sbomy@umd.edu

Even though the cell-based topology optimization has been attractive as a working tool for structural optimization, an extra work is needed to obtain smooth boundaries for practical applications. Several techniques of postprocessing the cell-based result to obtain a structural model with parameterized boundary are found in [19,30]. Several methods of topology optimization dealing with smooth boundaries have been performed, including the "bubble method" by Eschenauer et al. [10]. They defined a charac-teristic function to determine the optimal position of a hole which is rendered by a geometric function. The level set method [26], the technique to represent the propagation of boundaries at the zero-level of a level set function in a Hamilton-Jacobi type equation, was utilized for shape optimization [1,34]. Recently, the level set method is successfully combined with the topological derivative so that a topology change (hole generation) can be evoked [1-3, 6, 21, 26, 34]. Because these methods deal with the change of the boundaries, the result ensures smooth boundary and uniform density, which are strong points.

In this paper, a new version of topology optimization using explicit boundary representation and a new criterion for hole generation is proposed for similar motivation. The idea is simple combining smooth boundary representation and hole generation capability utilizing topological sensitivity. Shape optimization with B-spline curves is the basic scheme for boundary evolution. The topology is improved by either creating a hole in the domain or merging any two holes as shown in Fig. 1. After an optimization is complete, one has parametric information (location of the control points) allowing smooth boundary. Therefore, it is named "smooth boundary topology optimization (SBTO)."

Because SBTO is proposed under the same motivation with the level set method, the optimization results look similar.

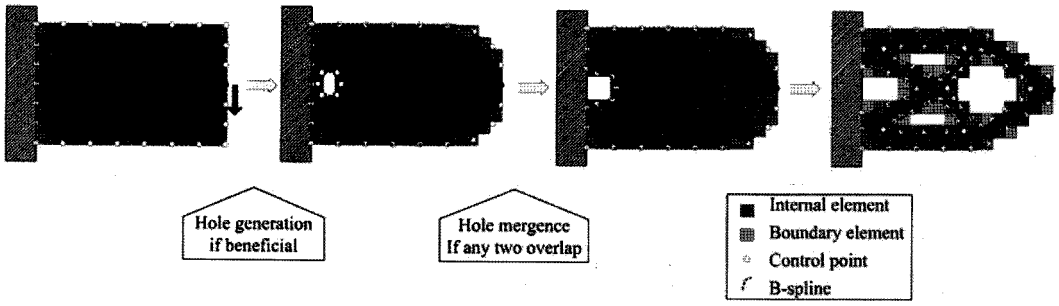

Fig. 1. Basic concept of SBTO.

The difference between them is discussed in Section 5. The content of this paper is as follows: In Section 2, the main concept of the proposed topology optimization is explained. In Section 3, several imple-mentation issues are discussed, such as constructing finite element model and setting up the move ranges of control points in shape optimization procedure. The feasibility of the methodology is shown in Section 4 with two examples.

2. Method

The main procedure is basically shape optimization using B-spline. All control points of B-spline are free to move in an achievable zone (D in Fig. 2 (a)). "Nonpenetrating zone (D^C)" is a zone where no entrance of a control point is allowed and indicated by a cross-hatched area. The procedure brings in a new topology when (1) a hole is generated or (2) any two boundaries merge and thus the number of design variables changes. For the second case, one can change the topology easily by checking intersection; if any two boundaries intersect, the control points of the overlapped part are wiped out and a new boundary is reformed as shown in Fig. 2 (c). For the first case (hole generation, Fig. 2 (b)), however, a quantitative scheme is necessary to compute the influence of making a hole on the design performance. A selection criterion, SC, is introduced for this purpose which is explained in the following section.

2.1. Selection criterion

In a minimization problem with one inequality constraint, a selection criterion (SC) is defined as the sensitivity of the objective function divided by the sensitivity of the constraint with respect to design variable b_i as follows:

$$SC_i = -\left.\frac{\psi'}{g'}\right|_i .$$

$\psi'|_i$ and $g'|_i$ are the design sensitivity of the objective function and the inequality constraint, respectively. SC_i indicates the ratio of the improvement in the objective function to the sacrifice in the inequality constraint due to a change in design variable b_i. In most normal cases, inequality constraints and the objective function behave in opposite direction, and SC normally has a positive value: In the case of the compliance minimization, for example, the objective function (compliance) increases and the constraint (typically volume) decreases when material is removed.

A physical meaning of SC is illustrated in Fig. 3. The horizontal axis is for design variable, b, and the vertical axis for function values. The origin of the graph indicates the current design. The function values of the objective function and the constraint may be different but are drawn at the same position. The angle between the horizontal axis and the arrow indicates the sensitivity value of the objective function and the constraint,

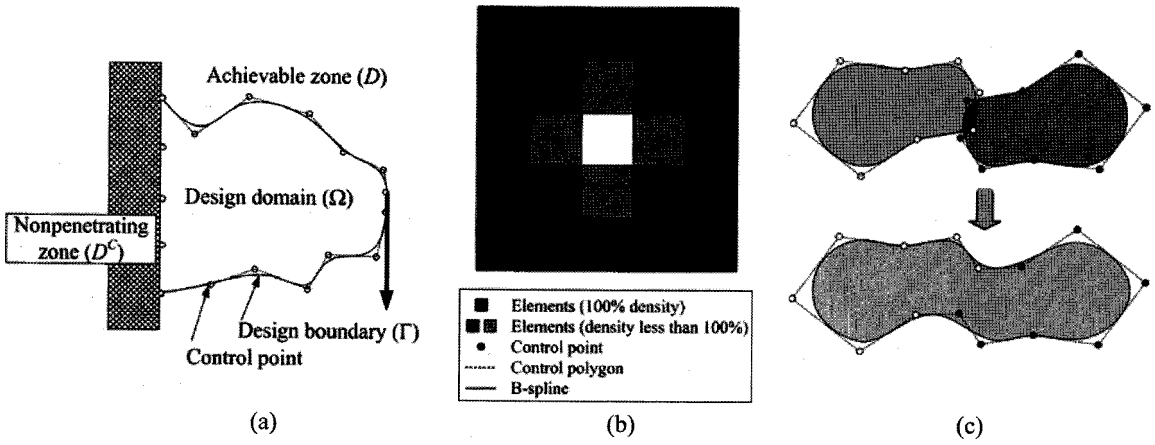

Fig. 2. Implementation of SBTO. (a) Domain setting, (b) Implementing topology change (hole generation), (c) (hole mergence).

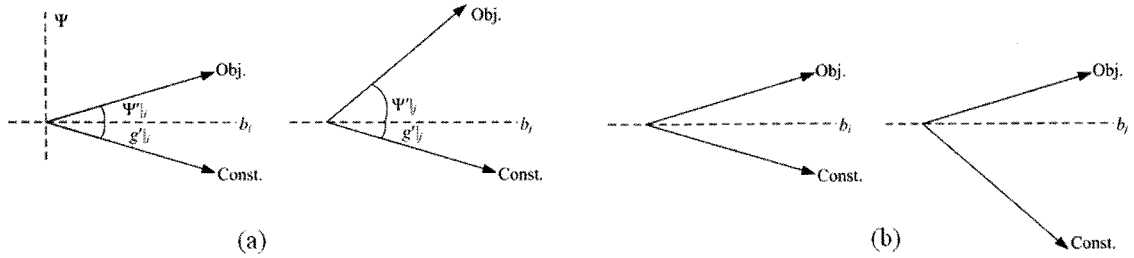

Fig. 3. Physical concept on selection criterion.

marked by $\psi'|_i$ and $g'|_i$, respectively. In Fig. 3 (a), for any two design variables (b_i and b_j), the case where $g'|_i = g'|_j$ and $\psi'|_i < \psi'|_j$ is investigated. In the minimization problem, we must avoid a rise of Ψ, and b_i is taken as a better way of design improvement ($SC_i < SC_j$). In the case of $\psi'|_i = \psi'|_j$ and $g'|_i > g'|_j$ (Fig. 3 (b)), on the other hand, we take b_j because a drop of g is the beneficial decision when the upper limit for the constraint exists (the volume must be less than a specified quantity, for example). In this case, $SC_i > SC_j$. To summarize, the smaller SC is taken for design improvement in both cases.

Consider a finite element model composed of M internal finite elements and its design boundary using a set of control points of B-spline (the sum of total degrees of freedom is NDV, the number of design variables). An internal finite element denotes a finite element not connected to the design boundary. Every iteration two kinds of SCs are calculated as follows:

$$SC_m^{\text{hole}} = -\left.\frac{\psi'}{g'}\right|_i^{\text{hole}}, \qquad m = 1,...,M,$$

$$SC_i^{\text{shape}} = -\left.\frac{\psi'}{g'}\right|_i^{\text{shape}}, \qquad i = 1,...,NDV, \tag{2}$$

SC_m^{hole} and SC_i^{shape} refer to the topological sensitivity ratio when a new hole is generated at the m-th element and the shape sensitivity ratio when the i-th design variable from control points moves, respectively. Because the smaller SC is taken for a better design, $SC_{\min}^{\text{hole}} = \min_m(SC_m^{\text{hole}})$ and $SC_i^{\text{shape}} \equiv \min_i(SC_i^{\text{shape}})$ are compared. If $SC_{\min}^{\text{hole}} > SC_{\min}^{\text{shape}}$, a boundary modification is regarded as the more advantageous way. In this case, one does not change the topology and continue shape optimization with the given control points. If $SC_{\min}^{\text{hole}} < SC_{\min}^{\text{shape}}$, however, it is judged that making a new hole is the more advantageous way which changes the topology of the domain.

2.2 Sensitivity analysis

During the optimization procedure of SBTO, two kinds of design sensitivities are calculated: the topological sensitivity and the shape sensitivity with respect to the B-spline's control points. The sensitivity for compliance in two-dimensional elasticity system is mainly concerned in this paper.

A topological sensitivity is introduced in [27], and derived by an application of the asymptotic analysis in singularly perturbed geometrical domains for a class of elliptic equations including the two-dimensional elasticity system [27] and three-dimensional elasticity system [28]. Recently, an alternative way is proposed to compute the topological derivative based on the shape sensitivity analysis concepts in [22,23]. These studies mainly focus on the topological derivative with respect to a void, which provides information about the variation of the shape functional due to creation of a small hole. The topological sensitivity can be also proved with the help of a domain truncation technique [11]. In this paper, the topological sensitivity formulation in [23] is taken among them and the topological sensitivity for compliance (or total potential energy) in two-dimensional elasticity system is given as follows (Neumann boundary condition on the boundary of the hole):

$$\psi' = \frac{2}{1+\nu}\sigma\cdot\varepsilon + \frac{3\nu-1}{2(1-\nu^2)} tr\sigma\cdot tr\varepsilon \tag{3}$$

where σ and ε are stress and strain tensor, and ν Poisson's ratio.

The shape sensitivity with respect to a B-spline control point is obtained by replacing the velocity field in the sensitivity formulation with the curve change of B-spline. A pth-degree B-spline curve is defined as follows [25]:

$$C(u) - \sum_{k=0}^{c} N_{k,p}(u) P_k$$

where P_k are the control points, $N_{k,p}(u)$ are the pth-degree B-spline basis functions ($p = 2$ is chosen in this paper), and u is knot variable. Let $U = \{u_0,..,u_m\}$ be a nondecreasing sequence of real numbers, i.e. $u_r < u_{r+1}$, $r = 0, \ldots, m-1$. The u_r are called knots, and U is a knot vector. The direct differential of Eq. (4) is substituted for the velocity field in the shape sensitivity formula from [12], and the shape sensitivity with respect to the B-spline control point is obtained as follows [17]:

$$\Psi' = \sum_{k=0}^{c}\left[-\int_{u_0}^{u_e}\left\{ \sum_{i,j=1}^{2} \sigma\cdot\varepsilon \right\} N_{k,p}(u) J du \right] \delta P_k$$

where J is Jacobian (dx/du), u_0 and u_e are knot variables corresponding to the starting and end point, respectively.

2.3 Optimization procedure

The optimization steps are summarized as follows:

Step 1 : Represent the initial design domain with several control points of the B-spline boundary.
Step 2 : Select design variables (movable control points).
Step 3 : Assign move ranges of the design variables.
Step 4 : Perform an iteration of shape optimization (by sequential quadratic programming, SQP) to find the new locations of the control points selected in Step 2.
Step 5 : If any two separate boundaries interfere, perform merge operation and go to Step 2. Otherwise, go to Step 6.
Step 6 : Calculate design sensitivity and compare SC^{hole} and SC^{shape}. If $SC^{hole}_{min} < SC^{shape}_{min}$, create a new hole with a new set of control points and go to Step 2 (see Fig. 2 (b)). Otherwise, go to Step 7.
Step 7 : Check convergence and side constraints (move ranges). Go to Step 3 if the optimization is not converged or there exists an active side constraint that does not meet a nonpenetrating condition (the case that additional design improvement is possible.). Terminate the optimization otherwise.

3. Issues for implementation

3.1 Fixed grids

The finite element model of "fixed grids" is used instead of automatically generated mesh. The uniformly distributed squares which cover the design domain (Ω) form the finite elements as shown in Fig. 4. For the element that overlaps a boundary, the concept of "NIO element" in FG ESO [15] is used; the density ρ is designated using the equations in Fig. 4 where ρ_0 is the material density of internal elements. The fixed grid has the advantage that it takes less time to generate a finite element model than an automatic mesh generation.

3.2 Move ranges setting

Much literature is found on the use of B-splines for shape optimization; nevertheless, they are mainly concerned with the movement of a few control points or only the change of a segmented boundary. In this paper, however, the sensitivity of every control point is investigated so that a drastic and overall change of the domain shape is possible. The problem during the shape optimization is that the design boundary of the B-spline could get entangled while each control point is seeking for an optimal position. In order to prevent this, move ranges are assigned for every control point (Step 3 in Section 2.3).

Fig. 5 shows a way to set up move ranges adopted in this paper. The control points are divided into groups, each of which represents a separate closed B-spline. A move range of a control point (P_0) is assigned, after finding the closest control point in the same group (P_1 in Fig. 5 (a)), with a side length of

$$L_0 = R \times \max(|\sin\theta|, |\cos\theta|). \tag{6}$$

R is the distance between the current control point (P_0) and the closest control point (P_1), and θ is the angle between the horizontal line and the line P_0P_1. Some move ranges are shown in Fig. 5 (b). The control points in the same group are considered finding the closest one (P_1) because this bound is only for prevention of any entangling. The move range for point P_i is repeatedly updated every iteration according to the following equation:

$$\begin{aligned} Pl_i^x &= P_i^x - 0.5 \times L_i, Pu_i^x = P_i^x + 0.5 \times L_i, \\ Pl_i^y &= P_i^y - 0.5 \times L_i, Pu_i^y = P_i^x + 0.5 \times L_i, \end{aligned} \tag{7}$$

where P_i^x and P_i^y are the x and y coordinate, Pl_i^x and Pu_i^x the lower and upper bound of P_i^x, and Pl_i^y and Pu_i^y the lower and upper bound of P_i^y. In the case that a move range partly includes a nonpenetrating zone (D^C), it is reduced so that it does not penetrate D^C. For example, the move ranges for P_3 and P_6 in Fig. 5 (b) overlap D^C, and they reduce along x and y direction accordingly. It is noted that, for simplicity

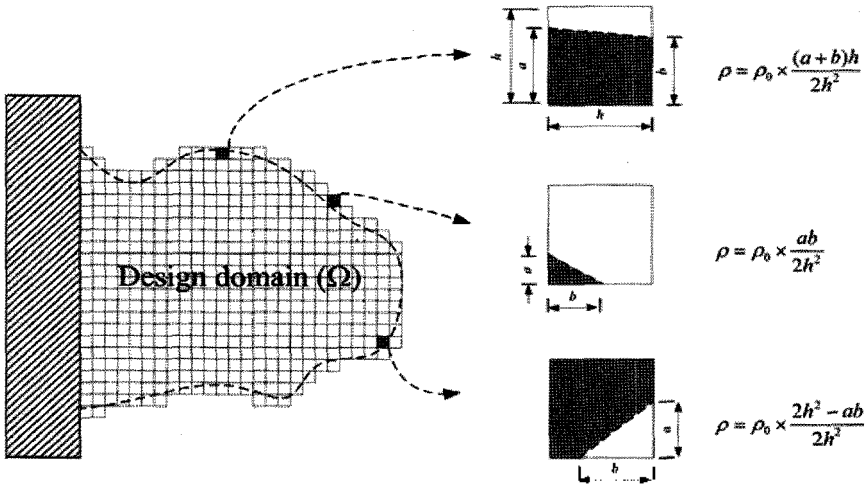

Fig. 4. Density for element overlapping boundary.

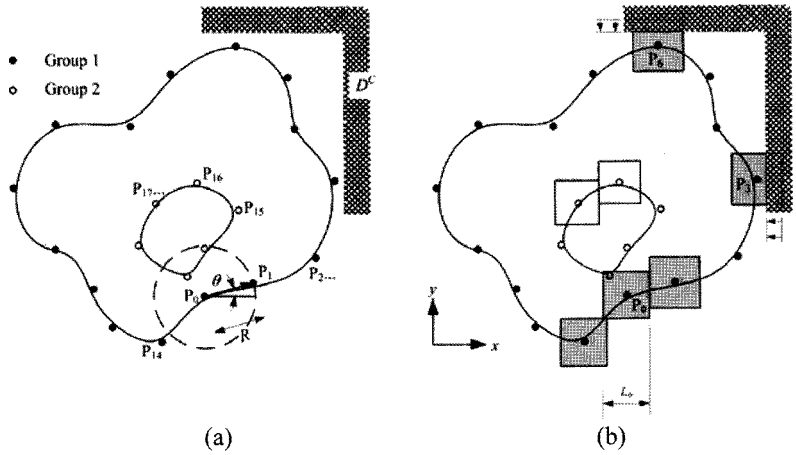

Fig. 5. Setting up move ranges.

of numerical implementation, any confliction of the nonpenetration constraint is checked by the nonpenetration of a control point instead of the curve itself.

4. Examples

The finite element analysis is done with ANSYS and PLANE42 element is chosen, and SQP algorithm in DOT [32] is used.

4.1 Short cantilever

The first example is design optimization of a short cantilever. The compliance is to be minimized and the volume is constrained to be less than 50% of its initial value. The left wall is fixed and a force of 100 N is applied downward at the center of the right edge as shown in Fig. 6 (a). The left wall is assigned as a nonpenetrating zone as shown in Fig. 6 (b). Two control points close to the loading point are fixed (black spots in Fig. 6 (b)), and they are not used as design variables. The control points attached to the left wall are restrained such that they can move only along the vertical direction. In this problem, a total of thirty five control points (total degrees of freedom is 51) with a 60 × 30 mesh are used in the initial model. The design optimization history is shown in Fig. 7.

In the beginning, a small hole near the middle of the left edge is created and soon merged with the left edge. Because only the left wall is designated as a nonpenetrating zone, control points can move anywhere except beyond this wall and the optimal design is obtained expanding out of the initial design domain, resulting in two bar truss structure with the volume constraint satisfied. The objective function, compliance, is reduced from 3.750 to 1.710 J.

Fig. 7 (b) shows the optimization history chart. The value of the objective function (compliance) and the constraint (volume) together with the number of design variables are shown in this chart. The objective function refers to the percentage value with respect to the initial volume. The constraint is divided by its initial value and 1 is subtracted, and the constraint is violated if this value is positive. DOT recognizes a constraint to be violated numerically if its value exceeds a prescribed tolerance of 0.003 [32], which is indicated as the dotted horizontal line in the chart. The curves for the objective function and the constraint are disconnected in the pivot phases, where a new hole is generated, or any two holes are merged (Step 5 and 6 in Section 2.3). In this case the number of design variables changes. The objective function and constraint lines are also disconnected when the move ranges are reset after the shape optimization is converged (Step 7 in Section 2.3). In this case the number of design variables does not change. Initially the number of design variables is 51, reaches up to 152, and finally ends up with 59. The optimization process is converged to have 45.6% of its initial compliance with the constraint satisfied after 46 pivot phases.

For this problem, a hole size of a finite element is a possible choice; One can find from the chart that there is little change

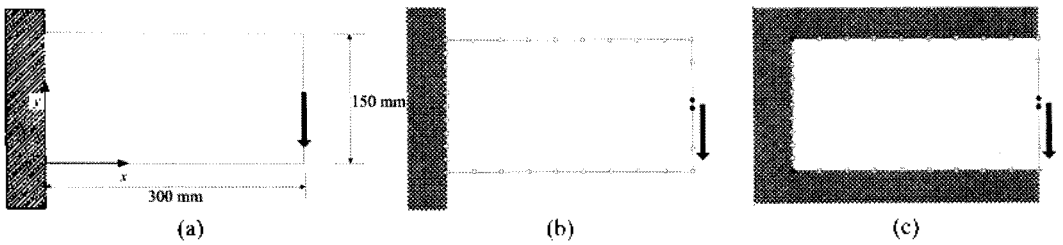

Fig. 6. Cantilever problem. (a) boundary condition, (b) nonpepentrating zone set 1, (c) nonpepentrating zone set 2.

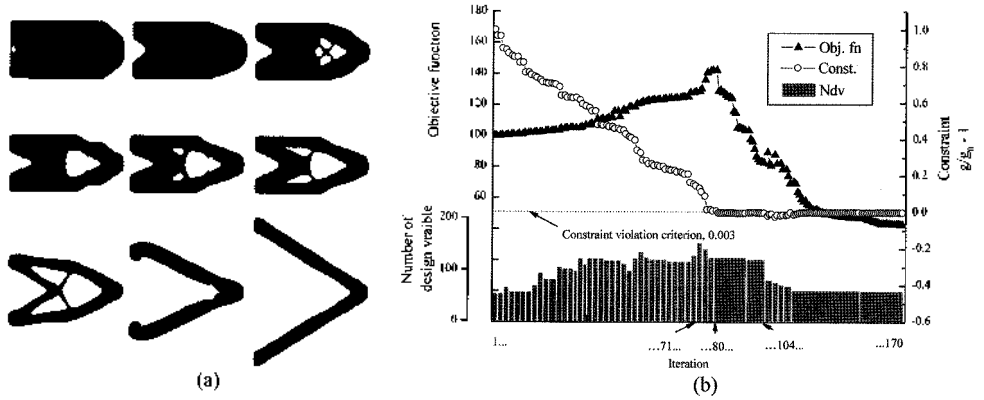

Fig. 7. Optimization history for nonpenetrating zone set 1.

on the functional values when a hole is generated (maximum change on the objective function is 0.13% at the 71st step.). At the 104th step, several holes are merged at the same time with about 6.6 % of the change on the objective function, which is the maximum among hole-merging cases.

The same problem is solved with a different setting of nonpenetrating zone: the upper and lower walls are added as non-penetrating zones (Fig. 6 (c)). In this problem, the compliance is increased to 5.158 J. This shows that the volume is constrained but there is little allowance for better arrangement of the material to reduce the compliance lower than the initial. The design procedure and the optimization history chart are shown in Fig. 8. At the beginning, it follows almost the same history as the first half of the first problem and converges at 138% of the initial objective function value with 118 design variables. The computation is done with an Intel Pentium 4 processor (2.40 GHz), and the total calculation time is 70 and 28 minutes, respectively.

4.2 Hip prosthesis stem design

Topology optimization of hip prosthesis stems is motivated as a practical case. Stress shielding is an important factor for stem design. This often occurs in the cortical bone adjacent to the femoral stem due to the difference in the elastic moduli of bone and prosthesis. Any large difference in stiffness causes a reduction of the tension/compression load or bending moment to the part of the bone and decreases bone masses [20]. This weakens fixation between the bone and prosthesis, and can be a cause of a revisiting surgery. Even after titanium was introduced as a biocom-patible excellent material, there is still the problem of finding an optimal shape of hip prosthesis to reduce the stress shielding [13,14,16]. Huiskes and Boeklagen [13] performed numerical shape optimization on an artificial hip joint, to reduce a weighted sum of strain-energy density (SED) along the cement/bone interface.

Topology optimization is now proposed as a new design concept. For the stem, holes should be allowed. This can enhance fixation due to the cement filled in the holes. Reflecting this purpose, a new optimization formulation is made considering the following two aspects: To generate holes to enhance fixation, and to reduce the volume for light structure.

4.2.1 Problem definition

Three different loading cases for hip prosthesis are described by Kowalczyk [16] which are a stance phase of gait and two extreme situations during normal activities. In the simplified model, only the joint head force is considered which is applied at the head pin. The joint force data are summarized in Table 1 and Fig. 9 (b).

The hip replacement model with cement is usually composed of three different parts: hip prosthesis stem, the cement layer, and the cortical bone. In order to use the sensitivity

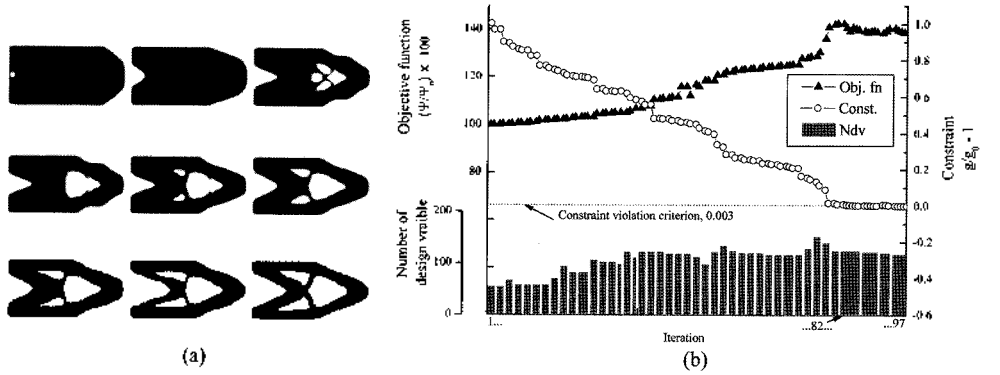

Fig. 8. Optimization history for nonpenetrating zone set 2.

formulation of Eq. (3) and Eq. (5), however, only the stem part is modeled replacing the others with some equivalent boundary conditions. Considering each loading case, the boundary condition is found by trial and error such that the distributions of von-Mises stress/strain and shear stress/strain remain similar. In the present paper, it is determined so that the stem has bending almost the same as the original model; all the y-directional nodal displacements at the bottom and the x-directional displace-ment at the midpoint of the right edge are fixed as shown in Fig. 9 (b).

For the new hip prosthesis to be designed, generation of holes should be included to enhance fixation. The stiffness of the structure need not be large because biomechanical alloys are adequately stiff compared with bone. Therefore, instead of minimizing compliance as done for usual formulations of structural design, the optimization problem is now defined to minimize volume (to induce hole generation) while keeping the compliance to be less than its initial value:

$$\min \Psi = \text{Volume}$$

Table 1. Numerical data for loads; angle is measured from the horizontal axis

Loading cases	Joint force	
	Value (N)	Angle (deg)
Stance phase (F_1)	2317	-104
Extreme case 1 (F_2)	1158	-75
Extreme case 2 (F_3)	1548	-146

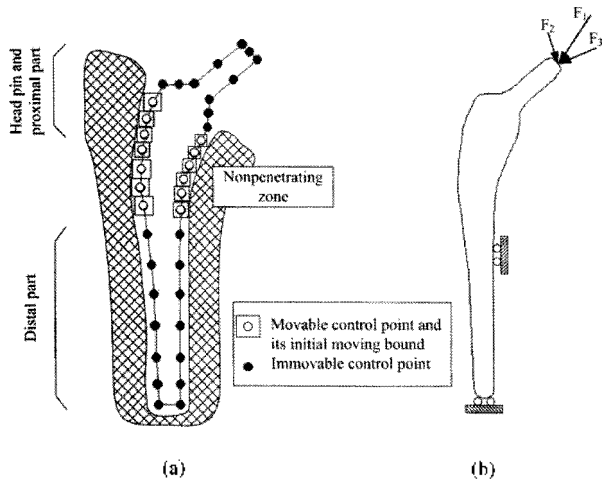

Fig. 9. Initial model and boundary conditions.

$$\text{s. t, } g = \text{Compliance} \le g_0$$

where g_0 is the initial compliance of the structure.

4.2.2 Model description

Fig. 9 (a) shows the initial model for the topology optimization. A total of 38 control points are used to render the initial design boundary. Because it is desired to retain a wide proximal part in order to prevent stress shielding [13, 14, 16], 11 control points around the head pin and the proximal part are fixed. The 14 control points in the distal part are also fixed to maintain its tapered shape which enables an easy insertion of the stem and prohibits unexpected air insertion [9]. The initial move ranges for the 13 movable control points are set by Eq. (7). In this problem, a non-penetrating zone as shown in Fig. 9 (a) is assigned in the cortical bone; the design boundary is not allowed to penetrate this region. The three loading cases (Table 2) are used in this optimization.

4.2.3 Results

Fig. 10 (a) shows the optimization history for the first loading case, F_1. The value of the objective function (volume) and the constraint (compliance) together with the number of design variables are shown in this chart. Initially the number of design variables is 26, reaches up to 52, and finally ends up with 48. The optimization process is converged to have 85.4% of its initial volume with the constraint satisfied after 15 pivot phases. The total calculation time is 29 minutes under the same computation environment with Section 4.1.

The results for different loading cases are shown in Fig. 10 (b). In the second example, the direction of the rib is almost coincident with the loading direction to support bending. In the third example, however, no hole is generated and the bellied shape in the middle part is obtained to support the axial load. It is shown that the hip prosthesis with holes is obtained when loads unparallel to the head pin are considered.

4.2.4 Discussion

To obtain meaningful results, varying loading conditions must be considered with more elaborate model of the total hip. The results obtained here have demonstrated feasibility of the SBTO as an applicable tool for complex systems. Also it is interesting to obtain a hip prosthesis with at least two holes as a new design.

Table 2. Comparison of SBTO and Level set method on shape optimization

Factors	SBTO (by B-spline)	Level set method
Updated information	B-spline's control points	Level set function value
Data sampling	nonuniform	uniform
Optimization engine	SQP	Level set equation
Updated information	B-spline's control points	Level set function
Re-initialization	No	Yes
Hole generation	Comparison of SCs	Insertion of soft material [6, 21] Adding a forcing term [3] Generating hole(s) periodically [2]

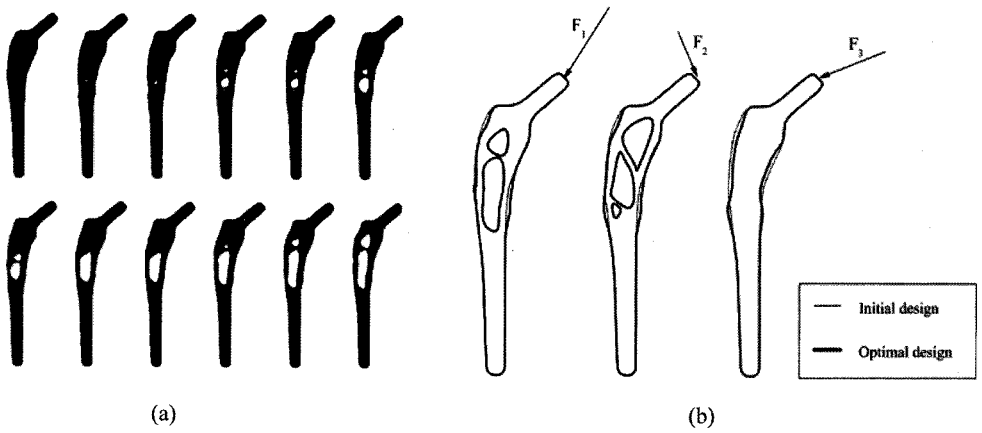

Fig. 10. Optimization result of hip prosthesis. (a) optimization history for the first loading case, (b) Comparison of the design for each loading case.

5. Comparison with the level set method

The excellence of the level set method to structural design problems has been reported in the literature [1-3, 6, 21, 26, 34] and it is worthwhile to compare with SBTO in this section for the following aspects: (1) boundary representation, and (2) combining with topological sensitivity.

5.1 Boundary representation

SBTO uses the parametric information (control points of B-spline) whereas the level set method represents the boundary implicitly by interpolating the level set function. In [8], the respective advantages and disadvantages of the two approaches of parametric and implicit contour representation are compared in terms of image process. Note that SBTO corresponds to the parametric representation. The main advantage of the implicit representation is obviously its ability to change automatically the contour topology during the deformation. This property makes it well-suited for reconstructing contours of complex geometry. Furthermore, on implicit contours the data-sampling is uniform and the resolution is constrained by the resolution of a regular grid.

One of the required steps in the level set method is the update of a narrow band around each contour. In fact, the update requires periodical re-initialization of the level set contour [1] to ensure that the level set function stays well-behaved; the level set function often becomes too steep to have a good approximation of the normal direction or of the curvature. A widely used way to this was given by [29]. Consider the partial differential equation

$$\phi_t = sign(\phi)(1-|\nabla\phi|), \tag{9}$$

where $sign(\phi)$ gives the sign of the level set function, ϕ. Given any initial data for ϕ, solving the above equation to steady-state provides a new value for ϕ with the property that $|\nabla\phi|=1$, since convergence occurs when the right-hand side is zero. The net effect is to "straighten out" the level set on either side of the zero level set and produce a ϕ function with $|\nabla\phi|=1$ corresponding to the signed-distance function. One potential disadvantage of the above scheme is that considerable motion of the zero level set can occur during the re-initialization [26], since the sign function is difficult to pinpoint the exact location of the front. Moreover, the frequency of the re-initialization is another issue to be determined, which may also affect the optimization result [33].

On representing boundary change using SBTO, the number and the location of control points can affect the result. In the current version, a "sufficient" number of control points are assigned in the initial model. When any two approach each other within the distance of a finite element size; the two points are considered as one. That is, one of them is taken out. Although only the meaningful control points remain and the others are "filtered out" through this elimination, a vertex sampling may not be uniform because no additional reallocation step is provided. Therefore, this number needs to be chosen rather carefully, to sufficiently represent boundary with appropriate DOF and not to spend too much time in optimization.

5.2 Hole generation

Recently, the generation of a hole is equipped in the level set method by combining with a topological sensitivity. Mei and Wang [21] incorporated the level set method and the multi-material topological sensitivity. In their research, the topological sensitivity describes the relative change ratio of the objective function when material is substituted in one point of the design domain. A similar approach is shown in [3], where the insertion of a soft material is considered in order to simulate a void. Burger et al. [6] included a forcing term in the Hamilton-Jacobi type equation in order to cause negative values of the level set function if it is favorable to add a hole at this position. The forcing term is chosen to be linearly dependent on the topological sensitivity, such that the topological sensitivity has higher influence where the topological sensitivity is negative in material. Allaire et al. [2] perform the hole generation from time to time and showed the frequency of the hole generation affects the optimization results.

In this paper, SC is introduced to decide the time for a

hole generation, which is defined by the ratio of the sensitivity of the objective function to the sensitivity of the constraint. Because SC^{hole} and SC^{shape} is compared every iteration, no user-defined parameter on the frequency of hole generation is required as used in the level set method. These points are summarized in Table 2.

6. Conclusion

A concept of topology optimization named SBTO was presented. The main point is that one can do topology optimization not by finding the optimal density of each finite element but by finding the optimal location of each control point and creating a hole if decided beneficial by comparing SC values. This guarantees uniform density through the whole design domain and smooth boundary during and after optimization. Using this methodology, neither separate filtering nor image processing is necessary because there is no zigzag boundary or checkerboard pattern. Moreover, no user-defined parameter such as the frequency of re-initialization or hole generation is needed. The SBTO approach was successfully applied to two topology optimization problems, showing the attractiveness and the elegance of the new method.

A hole created with a small radius grows in most cases, but takes too much time. An idea of overshooting for a faster growth may be helpful. This is a future topic of research to make the method practically applicable.

Acknowledgements

This work was partially supported by Samsung endowment fund for Samsung Chair Professorship.

References

[1] Allaire, G., Jouve, F. and Toader, A. M. (2004), Structural optimization using sensitivity analysis and a level-set method, *Journal of Computational Physics* **194**, 363-393.

[2] Allaire, G., Jouve, F. and Toader, A. M. (2005), Structural optimization using topological and shape sensitivity via a level set method, *Control and Cybernetics* **34**(1), 59-80.

[3] Amstutz, S. and Andra, H. (2006), A new algorithm for topology optimization using a level-set method, *Journal of Computational Physics* **216**, 573-588.

[4] Bendsøe, M. P. and Kikuchi, N. (1988), Generating optimal topologies in structural design using a homogenization method, Comput. *Methods Appl. Mech. Engng.* **71**, 191-224.

[5] Bendsøe, M. P. and Sigmund, O. (2003), *Topology Optimization - Theory, Methods and Applications*, Springer-Verlag.

[6] Burger, M., Hackl, B. and Ring, W. (2004), Incorporating topological derivatives into level set methods, *Journal of Computational Physics* **194**, 344-362.

[7] Chu, D. N., Xie, Y. M., Hira, A. and Steven, G. P. (1996), Evolutionary structural optimization for problems with stiffness constraints, *Finite Elements in Analysis and Design* **21**, 239-251.

[8] Delingette, H. and Montagnat, J. (2001), Shape and Topology Constraints on Parametric Active Contours, *Computer Vision and Image Understanding* **83**, 140-171.

[9] Dowson, D. and Wright, V. (1981), *An Introduction to the Bio-mechanics of Joints and Joint Replacement*, Mechanical engineering publications.

[10] Eschenauer, H. A., Kobelev, V. V. and Schumacher, A. (1994), Bubble method for topology and shape optimization of structures, *Structural Optimization* **8**, 42-51.

[11] Garreau, S., Guillaume, Ph. and Masmoudi, M. (2001), The topological asymptotic for PDE systems: the elasticity case, *SIAM J. Control Optim.* **39**(6), 1756-1778.

[12] Haug, E. J., Choi, K. and Komkov, V. (1986), *Design Sensitivity Analysis of Structural Systems*, Academic Press.

[13] Huiskes, R. and Boeklagen, R. (1989), Mathematical shape optimization of hip prosthesis design, *J. Biomechanics* **22**(8/9), 793-804.

[14] Katoozian, H. and Davy, D. T. (2000), Effects of loading conditions and objective function on three dimensional shape optimization of femoral components of hip endoprostheses, *Medical Engineering and Physics* **22**, 243-251.

[15] Kim, H., Garcia, M. J., Querin, O. M. and Steven, G. P. (2000), Introduction of fixed grid in evolutionary structural optimisation, *Engineering Computations* **17**(4), 427-439.

[16] Kowalczyk, P. (2001), Design optimization of cementless femoral hip prostheses using finite element analysis, *J. Biomechanical Engineering - Transaction of the ASME* **123**, 396-402.

[17] Lee, S., Kim, I. and Kwak B. (2004), Continuum topology optimization, the 10th AIAA/ISSMO Multidisciplinary Analysis and Optimization Conference Proceedings.

[18] Li, Q., Steven, G. P. and Xie, Y. M. (1999), On equivalence between stress criterion and stiffness criterion in evolutionary structural optimization, *Structural Optimization* **18**(1), 67-73.

[19] Lin, C. Y. and Chao, L. S. (2000), Automated image interpretation for integrated topology and shape optimization, *Struct. Multidisc. Optim.* **20**, 125-137.

[20] Long, M. and Rack, H. J. (1998), Titanium alloys in total joint replacement - a materials science perspective, *Biomaterials* **19**(18), 1621-1639.

[21] Mei, Y. and Wang, X. (2004), level set method for structural topology optimization and its applications, *Advances in Engineering Software* **35**, 415-441.

[22] Novotny, A. A., Feijoo, R. A., Taroco, E. and Padra, C. (2003), Topological sensitivity analysis, *Comput. Methods Appl. Mech. Engrg.* **192**, 803-829.

[23] Novotny, A. A., Feijoo, R. A., Taroco, E. and Padra, C. (2002), Topological Optimization Via Shape Sensitivity Analysis Applied to 2D Elasticity, World congress on computational mechanics (WCCM) Proceedings.

[24] Pedersen, N. L. (2000), Maximization of eigenvalues using topology optimization, *Struct. Multidisc. Optim.* **20**, 2-11.

[25] Piegl, L. and Tiller, W. (1986), *The NURBS Book*, Springer.

[26] Sethian, J. A. (1996), *Level Set Methods: Evolving interfaces in geometry, fluid mechanics, computer vision, and materials science*, Cambridge University Press.

[27] Sokolowski, J. and Zochowski, A. (1999), On the topological derivative in shape optimization, SIAM *J. Control Optim.* **37**(4), 1251-1272.

[28] Sokolowski, J. and Zochowski, A. (2001), Topological derivatives of shape functionals for elasticity systems, *Mech Struct Mach* **29**, 331-49.

[29] Sussman M., Fatemiy, E., Smereka, P. and Osherx, S. (1998), An Improved Level Set Method for Incompressible Two-Phase Flows, *Computers & Fluids* **27**(5/6), 663-680.

[30] Tang, P. S. and Chang, K. H. (2001), Integration of topology and shape optimization for design of structural components, *Struct. Multidisc. Optim.* **22**, 65-82.

[31] Tanskanen, P. (2002), The evolutionary structural optimization method: theoretical aspects, *Comput. Methods Appl. Mech. Engrg.* **191**, 5485-5498.
[32] VR&D. (1995), DOT users manual (version 4.20), Vanderplaats research & development, Inc.
[33] Wang, M. Y. and Peng, W. (2005), Topology Optimization with Level Set Method Incorporating Topological Derivative, 6th World Congresses of Structural and Multidisciplinary Optimization (WCSMO6) Proceedings.
[34] Wang, M. Y., Wang, X. and Guo, D. (2003), A level set method for structural topology optimization, *Comput. Methods Appl. Mech. Engrg.* **192**, 227-246.
[35] Xie, Y. M. and Steven, G. P. (1993), A simple evolutionary procedure for structural optimization, *Computers & Structures* **49**(5), 885-896.
[36] Yang, R. J. and Chuang, C. H. (1994), Optimal topology design using linear programming, *Computers & Structures* **52**, 265-275.

Soobum Lee is a postdoctoral research associate in the university of Maryland, U.S. He received the B.S. degree in Mechanical Design and Production Engineering from Yonsei University, Seoul, Korea, in 1998, and the M.S. and Ph.D. degree in Mechanical Engineering from KAIST (Korea Advanced Institute of Science and Technology), Korea, in 2000. His main research interests include structural shape and topology optimization, energy harvester design, nuclear plant design for hydrogen production, robust design using Taguchi method, genetic algorithm, automobile part and system design. He received the best paper award from Korean Society of Mechanical Engineering in 2007.

Byung Man Kwak is Samsung chair professor in the Department of Mechanical Engineering of KAIST, Korea. He received the B.S. and M.S. degrees in Mechanical Engineering from Seoul National University, Seoul, Korea, in 1967 and 1971, respectively, and the Ph.D degree in Mechanics and Hydraulics from the University of Iowa, Iowa City, in 1974. His main research interests are optimal design (shape, topology, and reliability based design optimization), contact mechanics, and design methodologies for development of practical systems. He has published more than 370 articles including 93 international journal papers listed in SCI, 37 domestic journal papers, 4 patents, 4 software registrations and 5 books and book chapters. He is a recipient of the 6th Korea Engineering Prize, a Presidential Award in 2005. Prof. Kwak is the elected Secretary General of International Society for Structural and Multidisciplinary Optimization (ISSMO). He is associate editors of Mechanics based Design of Structures and Machines, and Journal of Structural and Multidisciplinary Optimization. He is a fellow of American Society of Mechanical Engineers (ASME), and former president of Korean Society of Mechanical Engineers. He is registered in Marquis Who's Who in the World, in Asia, 2000 Outstanding Intellectuals of the 21st Century by International Biographical Centre, and in American Biographical Institute.

Il Yong Kim is an Assistant Professor in the Department of Mechanical and Materials Engineering at Queen's University, Ontario, Canada. He received the M.S. and Ph.D. degrees in mechanical engineering from the Korea Advanced Institute of Science and Technology (KAIST). He worked as a postdoctoral researcher in the Department of Aeronautics and Astronautics at the Massachusetts Institute of Technology. His research interest is Multidisciplinary System Design Optimization with applications in automotive and bioengineering systems. He received a number of awards including the best paper prize at KAIST and the Silver medal at 7th Samsung Electronics International Paper Competition.

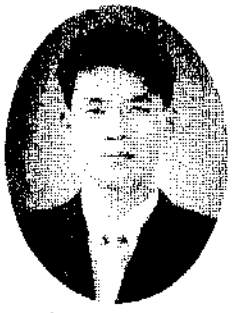
Soobum Lee


Byung Man Kwak


Il Yong Kim